Converting weather radar data to Cartesian space: A new approach using DISPLACE averaging

Marion P Mittermaier* and Deon E Terblanche
Bethlehem Precipitation Research Project, Weather Bureau, Private Bag X15, Bethlehem 9700, South Africa

Abstract

Volume-scan radar data can be processed to display radar rainfall fields on constant altitude planes. These displays are called CAPPIs. A new interpolation method is described and the CAPPIs so produced are compared to those obtained using conventional schemes. The new method is called DISPLACE Variate Averaging or DVA and is computationally efficient, requiring only half the computer time of other interpolation methods. DVA avoids division and multiplication and many of the conversions between units. It therefore provides new possibilities for real-time CAPPI processing. The method's output is used to compile rain fields for convective showers and general rain conditions which occurred during February 1996, using the data from an S-band radar.

Introduction

Constant Altitude Plan Position Indicators (CAPPIs) are an important radar-data derived product in the field of hydrometeorology. A large portion of South Africa's rainfall is produced by convective storms which are characterised by rainfall fields with high spatial and temporal variability. The representativeness of point measurements provided by rain gauges becomes very limited for convective rainfall. Doviak and Zrnic (1984) commented on the problem indicating the inverse relationship between the percentage error in using rain gauges to estimate area rainfall and the true areal mean rain depth. Seed (1993) noted that the rain-gauge measured rainfall is at best representative of a 10 km^2 area. Astute water resource management is required to meet the growing demands of the community. This need has focused attention on the use of area rainfall estimation, since the nationwide rain-gauge network is too sparsely distributed for simple extrapolation methods to provide accurate area estimates. Radar provides a means to scan large volumes of the atmosphere at high resolution and to capture information on the intensity of the precipitating scatterers in real time. As rainfall stimulation research in South Africa (Mather and Terblanche, 1994) moves towards area experiments, away from individual convective cells as experimental units, the use of radar to verify the outcome becomes even more important.

Radar is often operated in volume-scan mode whereby a three-dimensional image of the precipitation scatterers is obtained by consecutively scanning the atmosphere at higher elevations for complete azimuthal rotations. However, the data captured during this process are in spherical co-ordinates which is not ideal for the purpose of data analyses. CAPPI-processing techniques can be classified into two broad groups, viz. projection and interpolation methods. The radial distance from the radar determines the elevation step(s) from which data will be utilised, i.e. data from progressively lower elevations will be used as the distance from the radar increases. This inverse relation holds irrespective of CAPPI height and method, although the data usage transition between elevations is abrupt in projection methods, and more gradual and smooth in interpolation methods.

The projection method, where data from a slant elevation plane are projected onto a horizontal plane parallel to the earth's surface has been very popular due to its relative simplicity. However, the method does have drawbacks. Discontinuities appear at ranges where the data-use transition between different elevations occur. These discontinuities are always present but are most evident in the presence of data collected in stratiform precipitation.

In the sections that follow, a brief background to radar meteorology with reference to the MRL5 dual-wavelength radar, the rain-gauge network in the Bethlehem area and the interpolation CAPPI procedures in use in South Africa, is given. This is followed by the derivation of the CAPPI equations with emphasis on the new DVA method of interpolation. Finally, the advantages and use of the procedure in compiling rainfall maps from the S-band section of the MRL5 radar, verified against surface measurements, are shown in a case study.

Equipment

Radar data processing and the MRL5 radar

The background to radar and its uses in meteorology is well described by Atlas (1990), Battan (1973) and Doviak and Zrnic (1984). A short summary of some of the relevant aspects is given below.

Conventional weather radars generally use logarithmic receivers to accommodate the large range of received powers (>10^6) from precipitation echoes. A range correction term introduces a further 10^2 increase to the received power range that has to be provided for. In addition, the returned power from precipitation echoes exhibits a large sample-to-sample variance, necessitating averaging over a large number of samples to obtain accurate estimates of the mean received power. Before averaging, the analog signal from the logarithmic receiver (known as the video signal), is digitised to derive video processor (VP) counts. These are integer values reflecting the resolution of the analog to digital converter used (e.g. 12 bits). The averaged VP counts - which should be corrected for the bias (-2.5 dB) introduced by averaging the logarithms of the received power from precipitation echoes - can then be related back to the average received power (in dBm) through the calibration slope of the specific radar

* To whom all correspondence should be addressed.
☎(058) 303-5571; fax (058) 303-2352; e-mail mpmitt@nprp8.ofs.gov.za
Received 11 March 1996; accepted in revised form 19 September 1996.

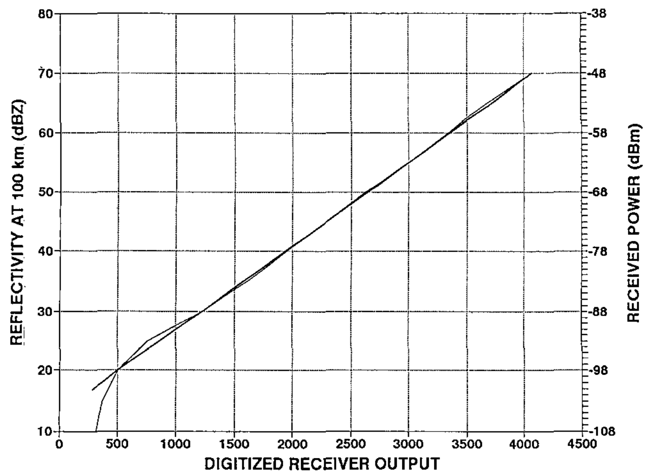

Figure 1
The calibration slope for the S-band receiver of the MRL5 radar. The bold line represents the slope which is used to convert video processor output (VP counts) to received power (dBm).

as shown in Fig. 1. The received power is then related to the reflectivity factor through the radar equation in logarithmic form:

$$10 \log P_r = 10 \log Z - 20 \log r + C \quad (1)$$

where P_r is the received power, Z the reflectivity factor, r the range and C the radar constant that includes all the radar-specific characteristics. The term 10 log Z is the well-known dBZ factor.

Marshall and Palmer (1948) found that the reflectivity factor, Z, can be related to the rain rate, R, in $mm{\cdot}h^{-1}$ through:

$$Z = 200R^{1.6} \quad (2)$$

This empirical relationship is just one of many that have been suggested for different conditions, locations and sampling wavelengths. Battan (1973) lists more than 60 of these relationships which is an indication that reflectivity alone does not describe a precipitation drop-size distribution explicitly. Fortunately, the drop-size distribution normally manifests itself exponentially allowing the use of the classic relationship given in Eq. (2).

A Russian-built MRL5 dual-wavelength weather radar operating at S- and X-band (10 cm and 3 cm wavelengths) was acquired by the Water Research Commission in 1994. This system was installed on a site 20 km northwest of Bethlehem and was upgraded to the computer-based Radar Data Acquisition System (RDAS) for antenna control, signal processing, display and storage described by Terblanche et al. (1994). Data for 224 range bins, each 600 m in length, averaged over 32 individual samples, are calculated for each degree of azimuth. A volume scan, which takes just less than 5 min to complete, consists of data from 18 elevations. In February 1995 the signal processing of the logarithmic receiver output was changed to the DISPLACE method of averaging (Terblanche, 1996) to obtain average reflectivity values simulating those that would be obtained from a quadratic receiver. In this manner, an unbiased estimate of the average received power is calculated for each range bin, thus not requiring the bias correction mentioned before.

Supporting infrastructure for radar rainfall studies

The Bethlehem precipitation research project (BPRP) deployed an extensive rain-gauge network of 71 tipping bucket rain gauges (TBRs) in the Bethlehem area using high resolution in-house developed event loggers (Van der Hoven and Kroese, 1995). Forty-five of these TBRs are situated within the Liebenbergsvlei River catchment and have a 10 km spatial resolution. The other 26 TBRs are situated within the Vaalbankspruit catchment, a subcatchment of the Wilge River. These rain gauges have a 4 km spatial resolution. The accuracy of measurement by the TBRs was verified through an automated calibration procedure described by Van der Hoven and Kroese (1995). The event loggers were designed to record, to the nearest second, each 0.2 mm of rain measured by the gauge. As stated previously, rain gauges only provide accurate point measurements of rainfall and therefore, there can be large differences between radar and rain-gauge rainfall measurement, especially for convective rainfall. Despite these limitations, rain gauges provide our only means to verify the measurements made by radar, the comparison being the most realistic under general rain conditions where one can integrate the fairly homogeneous rainfall field over both time and space.

CAPPI Processing Techniques used in South Africa

In South Africa a variety of CAPPI processing software is in use. The methods used by the BPRP are projection methods, providing data with a 1 km resolution and were originally intended for use under convective conditions alone. The method in current use was developed by Seed (1992) to track the rain areas and accumulate the rainfall from convective showers. More recently the BPRP obtained TITAN software, an acronym for Thunderstorm Identification, Tracking Analysis and Nowcasting, developed by Dixon and Wiener (1993). The TITAN CAPPIs have a 1 km resolution, and the CAPPI heights are referenced to mean sea level (m.s.l.).

The South African Weather Bureau (SAWB) developed an interpolation CAPPI method with a 2 km horizontal resolution for all the SAWB radars connected to the Central Forecasting Office (Visser and le Roux, 1993). The main restriction for interpolation methods has been computing power, which limited the number of CAPPIs to one set every other volume scan. This obstacle is now being rapidly eliminated by the high performance personal computers which are now available on the market.

Development of the DISPLACE variate averaging CAPPI method

Development of a conventional forward averaging scheme

Since no interpolation CAPPI method was operational within the BPRP, the first step was to develop and implement a conventional interpolation scheme similar to that described by Mohr and Vaughan (1978).

Grid generation and grid-point matching

A 200 km x 200 km window with 1 km resolution Cartesian co-ordinate grid (x, y, z) was transformed to radar co-ordinates of slant range (r), azimuth (θ), and elevation (ϕ), using

$$r = (x^2 + y^2 + z^2)^{0.5} \quad (3)$$

$$\theta = \arctan(x/y) \tag{4}$$

To calculate the elevation, an adjusted vertical co-ordinate is used:

$$z_h = z - ((x^2 + y^2) / aD) \tag{5}$$

where a is the standard compensating tropospheric beam refraction factor of 4/3 (Battan, 1973) and D the approximate earth's dia. The elevation angle is therefore:

$$\phi = \arcsin(z_h / r) \tag{6}$$

Since the Cartesian grid points and the radar data grid points do not necessarily match, weighting factors, reflecting these differences, are calculated to allow for the interpolation from the data points. The four radar data grid points closest to a Cartesian grid point were therefore identified on each constant elevation plane and the differences calculated. The distance between a CAPPI plane and the elevation plane heights was also calculated, to provide six weighting factors per Cartesian grid point.

Forward averaging scheme

The scheme comprises two weighted averaging equations. Firstly, radar data points undergo a horizontal interpolation on a constant elevation plane :

$$Z(r,\theta) = [1/(\Delta r \Delta\theta)]\ \{\underset{\mathbf{r_1}}{(r-r_i)}\ [\underset{\mathbf{az_1}}{(\theta-\theta_j)}\ z(i+1, j+1) - \underset{\mathbf{az_2}}{(\theta-\theta_{j+1})}\ z(i+1, j)] - \underset{\mathbf{r_2}}{(r-r_{i+1})}[(\theta-\theta_j)z(i+1, j) - (\theta-\theta_{j+1})z(i, j)]\} \tag{7}$$

where $\Delta r = 600$ m and $\Delta\theta = 1$ degree, $\mathbf{r_1}$ and $\mathbf{r_2}$ are the two range weighting factors, $\mathbf{az_1}$ and $\mathbf{az_2}$ the two azimuth weighting factors. Equation (7) is applied to two consecutive constant elevation planes reducing four data points to one representative point on each plane.

Next, inter-elevation plane interpolation:

$$Z(r,\theta,\phi) = (1/\Delta\phi)\ [\underset{\mathbf{el_1}}{(\phi-\phi_k)}\ Z(r,\theta,\phi_{k+1}) - \underset{\mathbf{el_2}}{(\phi-\phi_{k+1})}\ Z(r,\theta,\phi_k)] \tag{8}$$

where $\Delta\phi$ is the difference in degrees between consecutive radar elevation steps, $\mathbf{el_1}$ and $\mathbf{el_2}$ are the elevation weighting factors. Figure 2 is a graphical depiction to clarify Eqs. (7) and (8). The Cartesian and radar co-ordinates, together with the six weighting factors as indicated in the equations, are stored in grid look-up tables.

VP counts have to be converted to reflectivities (dBZ) via the radar calibration relationship and radar equation. To implement the method described in Eqs. (7) and (8) a further conversion to reflectivity factor (Z) using the log relation:

$$Z = 10^{(dBZ/10)} \tag{9}$$

is required. Only then can interpolation be performed. The interpolation output is then converted back to dBZ, using Eq. (9); or to rain rates using equation Eq. (2).

The simplification of the interpolation technique

The conventional averaging described in the previous section can be simplified. Both Eqs. (7) and (8) describe the process of calculating weighted averages of pairs of data points in Z-space (dBZ=10 log Z). Equation (7) entails calculating two weighted averages in azimuth at consecutive ranges and one in range. Equation (8) determines a weighted average between two data points calculated by Eq. (7). Each CAPPI grid point value to be determined requires the calculation of seven weighted averages of data point pairs.

From Terblanche (1996) the DISPLACE equation for obtaining an unbiased average, in dBm, from a pair of logarithmically received samples, $10 \log P_1$ and $10 \log P_2$ is given by:

$$10\log((P_1+P_2)/2) = 10\log P_1 - \mathbf{10\{\log 2 - \log[1+0.7943^{(10\log P1 - 10\log P2)}]\}} \tag{10}$$

where the bold section, a function of $10 \log P_1 - 10 \log P_2$, is known as the **displacement** value which must be applied to $10 \log P_1$. Applying the range correction term in (1), to the $10 \log P_i$ values results in the application of Eq. (10) to dBZ values. From Eq. (10) we can now obtain an equation for calculating an unbiased weighted average over a pair of dBZ values - the DVA equation:

$$10 \log\{[bZ_1+(1-b)Z_2]\} = (10 \log Z_1 + 10 \log b) + 10 \log\{1+0.7943^{[(10\log Z1+10\log b)-10\log Z2+10\log(1-b)]}\} \tag{11}$$

with $0<b<1$, the weighting factor.

The terms 10 log b and 10 log (1-b) now represent the weighting factors in dB which must be added to the data pair values, $10 \log Z_1$ and $10 \log Z_2$. All terms in Eq. (11), as well as the range correction term, can be scaled with the appropriate calibration slope to enable calculations to be done directly on VP counts. The decibel weighting factors are now stored in the grid look-up tables.

From Eq. (11) it can also be seen that in using DVA, the multiplications between weighting factors and data values in Eq. (7) and (8) are replaced with simple additions done on range-corrected VP counts, thus avoiding the time-consuming conversions to Z values. The averaging is accomplished in the following manner:

Consider any appropriate pair of range-corrected VP count values, VP_1 and VP_2, as identified in Eqs. (7) or (8), then:

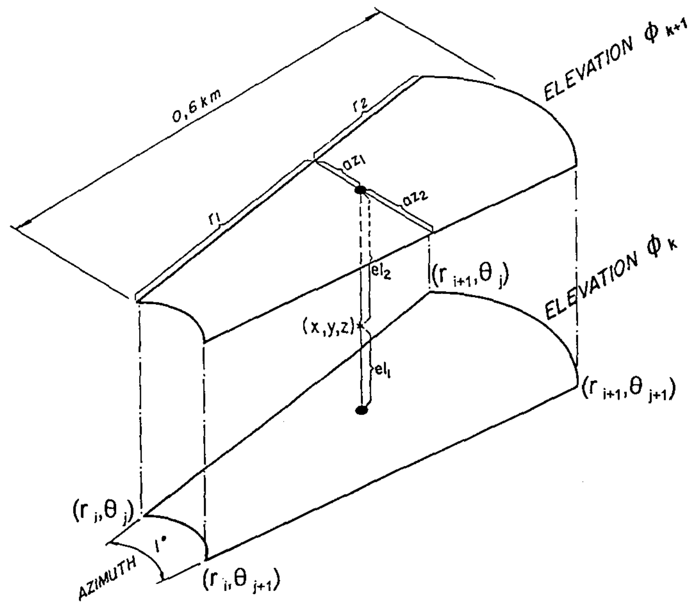

Figure 2

Diagram illustrating a Cartesian grid point and the eight radar data points surrounding it. Also indicated is the manner in which the weighting factors for interpolation are determined.

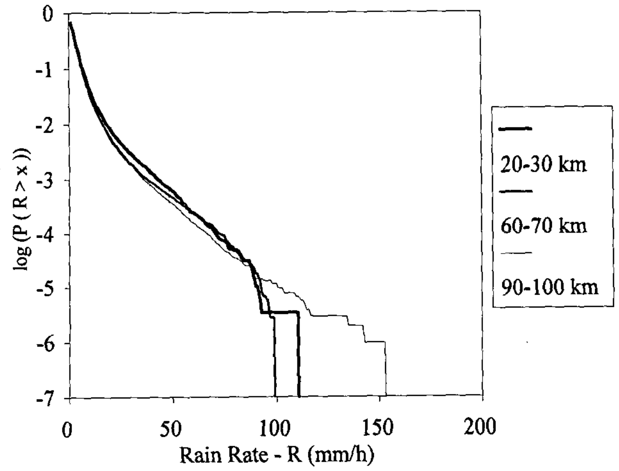

Figure 3
Rain-rate exceedance probabilities in three 10 km annuli for the period 9 to 16 February 1996.

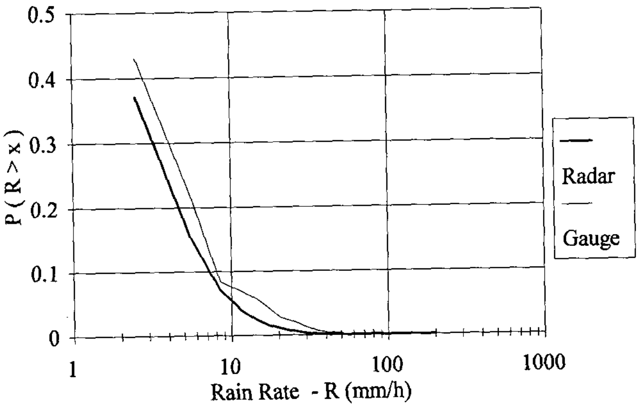

Figure 4
Radar and rain-gauge rain-rate exceedance probabilities for the Liebenbergsvlei River catchment for the 24 h period, 13 to 14 February 1996.

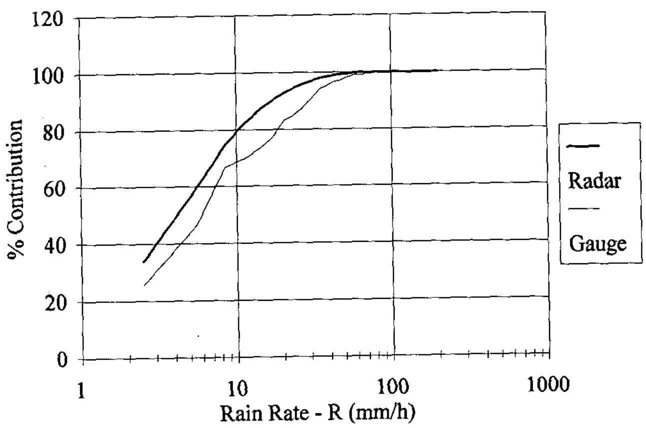

Figure 5
Cumulative radar and rain-gauge rain-rate contributions for the Liebenbergsvlei River catchment rainfall for the 24-h period, 13 to 14 February 1996.

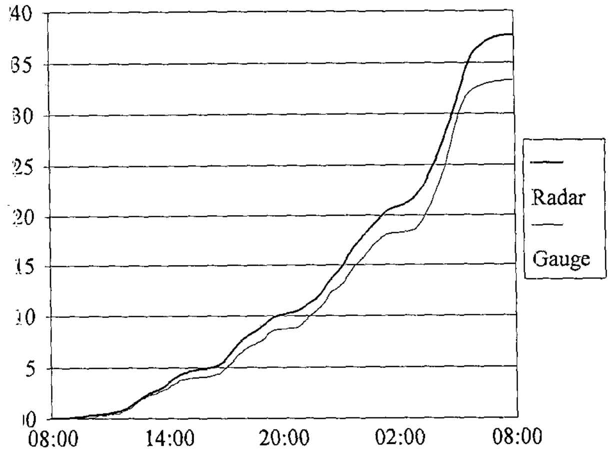

Figure 6
Time history of accumulated radar and rain-gauge rainfall for the Liebenbergsvlei River catchment for the 24-h period, 13 to 14 February 1996.

- Add the appropriate dB weighting factors to VP_1 and VP_2 to obtain VP_1' and VP_2'
- Calculate the difference between VP_1' and VP_2'
- Use the difference as a pointer in the displacement table
- Subtract the look-up table value from VP_1' to obtain the weighted average.

The final output can be converted to the desired units (dBZ or rain rate) using another look-up table based on the calibration relationship. Note that if the intention is to accumulate rainfall over a number of CAPPIs, the DISPLACE approach makes it possible to keep all values as VP counts, as the accumulation process consists once again of weighted averages.

Results

A comparison between the conventional and DVA methods

One of the reasons why interpolation CAPPI display methods have not been widely implemented in real time, was the time required to produce CAPPIs in this manner.

The software development done for this study was accomplished on an HP-9000-835 under UNIX using Fortran 77. To obtain an objective run-time comparison, two test programs were written to obtain the equivalent of a 200 x 200 pixel CAPPI using eight data points contributing to each pixel - one using the conventional method and the other DVA. The starting point in both cases was VP values and the result in dBZ values. It was found that the DVA method requires only half the computer CPU time of the conventional CAPPI interpolation method.

This improved efficiency can be ascribed to:

- the elimination of excessive data conversions between different units;
- the extensive use of look-up tables;
- the elimination of multiplication and division; and
- virtually the entire method being integer-based.

A case study - February 1996

In the period 9 to 16 February 1996, widespread heavy rain fell over the eastern parts of South Africa resulting in extensive

Figure 7
Accumulated 24 h rainfall field for 13-14 February 1996:
(a) 2 km DVA CAPPI-based data with isohyets inferred from the rain-gauge network as well as rainfall figures from daily stations and
(b) using Seed's method

flooding. DVA CAPPIs were computed for 2 km above ground level using S-band data from the MRL5 radar for the entire period.

A Cartesian grid point of the DVA CAPPI is compiled using data from a fixed number of range bins (eight). The dimensions of the range bins increase with range due to beam broadening, resulting in an increase of the sampled range-bin volume. Concern existed as to the range dependancy of rainfall statistics in that a progressive filtering of high rainfall rates might occur with distance. The method used by Seed (1992) was to calculate the average Z for all range bins that fell inside a Cartesian grid cell, thus ameliorating to some extent the sensitivity of rainfall statistics to areal averaging. DVA CAPPI rain-rate exceedance probalilities - per 1 mm·h^{-1} interval - were calculated for 10 km annular rings between 20 and 100 km in the northern sector of the radar for the period 9 to 16 February 1996. The southern sector was not included, avoiding the possible contamination of the rainfall statistics by ground clutter. This 7-d period was characterised by a combination of stratiform and convective rainfall. As shown in Fig. 3 the rain-rate statistics in the annular rings indicate no systematic change in the occurrence of high rainfall rates. Other studies have shown that the quadratic averaging of digitised receiver samples using the DISPLACE method (Terblanche, 1996) counteracts the exaggerated beam broadening effects of conventional averaging.

The radar measurement of widespread rain has not received much attention in South Africa. These conditions are characterised by shallow reflectivity profiles with large vertical gradients. Vertical gradients of reflectivity are the cause for the concentric discontinuities in projection CAPPIs. During the event under consideration, the vertical structure of the reflectivity profiles indicated the existence of a bright band (Battan, 1973), but at altitudes higher than the 2 km CAPPI level. Although the bright band did not have a severe impact on the results of this study, it is a feature of stratiform rain in South Africa that warrants further investigation. It has been found to lead to large over-estimations in radar rainfall under specific conditions.

The 24-h period starting at 08:00 SAST on 13 February 1996 was typical of the February rain event. In Fig. 4 the rain-rate exceedance probabilities using all the CAPPI grid pixels for the Liebenbergsvlei River Catchment (4 650

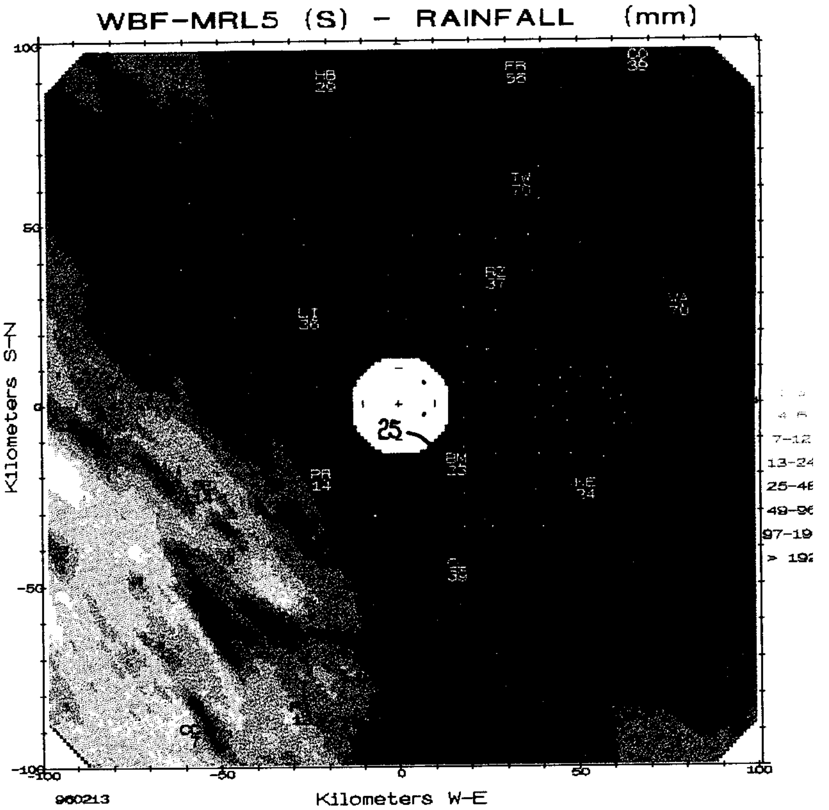

Scale : 1-3 4-6 7-12 13-24 25-48 49-96 mm

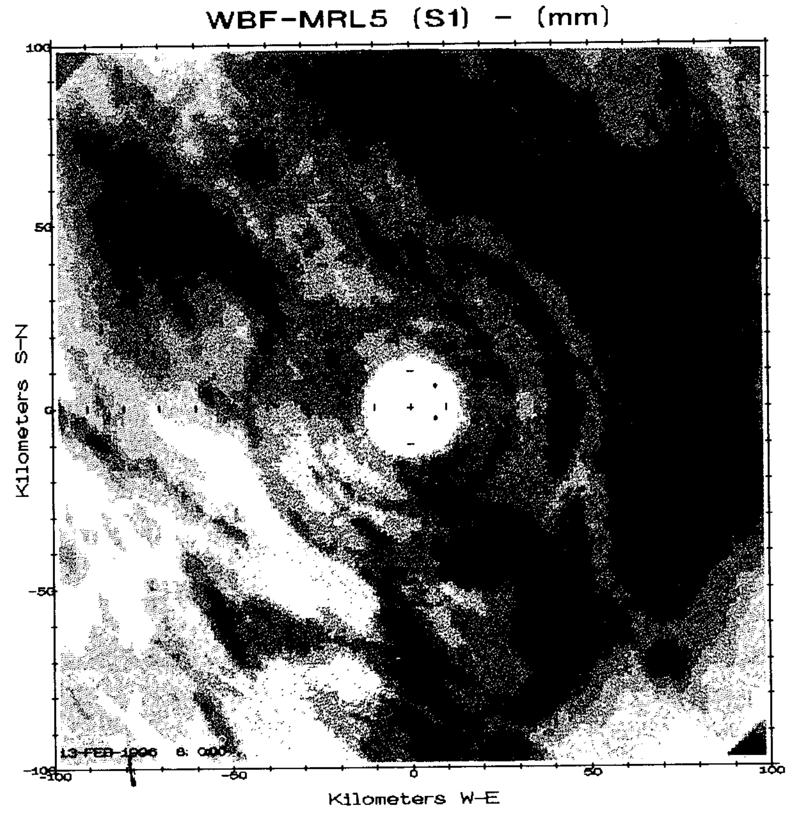

km^2) and the data from the 45 tipping-bucket rain gauges within the catchment are shown. For both data sets the rain rates refer to the volume-scan period (4.7 min) and are divided into 3 mm·h^{-1} intervals. The first interval is centred on 2.5 mm·h^{-1} which is the rain-rate measuring threshold of the rain gauges.

In Fig. 5 the cumulative rain-rate contribution using radar and rain-gauge data is shown for the same 24-h period. From both these figures the good radar-rain-gauge correspondence is apparent while the smoothness of the radar curves is an indication of the superior area sampling by radar.

The 24-h cumulative catchment rainfall inferred from radar and the rain-gauge network is shown in Fig. 6. The radar-rain-gauge ratio for this day is 1.12 compared to 1.03 for the total 7-d period. The average area rainfall for the total period was approximately 115 mm.

Figures 7(a) and 7(b) show the 24-h rainfall fields obtained by accumulating the 2 km DVA CAPPIs and using Seed's (1992) procedure at the same height. The isohyets (using intervals similar to those for the grey scale) for the total rain-gauge network as well as rainfall figures from daily reporting stations within the radar area are plotted on the DVA CAPPI field. The area of the 2 km CAPPI (to a range of approximately 75 km) is extended at larger ranges with base-scan data. A gradient in the rainfall field is clearly evident, with the north-eastern parts receiving the most rainfall. The ground clutter, in excess of 50 km from the radar in the south-eastern sector, is caused by echoes from the Rooiberge and the Lesotho mountains. Note the absence of concentric rainfall discontinuities in the DVA CAPPI field.

Conclusions

The DVA method of interpolation is twice as computationally efficient as conventional interpolation. This is a result of a decrease in radar data pre-processing which entails multiple unit conversions, as well as the elimination of multiplication and division. The DVA method improves radar-rainfall estimates, the rainfall statistics appear to be stable in range and the method eliminates the discontinuity rings characteristic of the current projection methods for widespread stratiform rain.

Radar data presented in the format described should prove invaluable in providing a systematic rain-field record over relevant time periods to aid flood forecasting and reservoir management. The accumulative rainfall fields allow for a holistic perception of a developing hydrological situation at a glance. Radar coverage over the high flood risk areas of South Africa, can be used beneficially to alert the relevant authorities of impending danger.

Accurate radar-determined rain fields will benefit the rainfall stimulation research, especially as the research moves closer to area-wide experimentation where a continuous record of the area rain field will become of crucial importance.

The MRL5 radar and the optimum use of the data from the system are under continual development. A system is now being introduced to generate eighteen DVA CAPPIs per volume scan on a personal computer (in C) at the MRL5 site. The output fields will be transmitted to Bethlehem in real time using a high-speed radio link. When completed, the system will facilitate the distribution of the data to many more end-users. Methods to filter the effects of ground clutter and the bright band are under way. The use of the dual-wavelength facility of the MRL5 to further improve radar-rainfall measurement and identify areas of hail have also been identified as further areas of research.

Acknowledgements

The authors would like to thank Dr Graeme Mather, Dennis Dicks and Karel de Waal for their valuable contributions. The support of the other members of the BPRP staff is greatly appreciated. This research was funded by the South African Weather Bureau (Department of Environment Affairs and Tourism) and the Water Research Commission as part of the National Precipitation Research Programme.

References

ATLAS D (1990) *Radar in Meteorology.* Battan Memorial and 40th Anniversary: Radar Meteorology Conference, AMS, USA.

BATTAN LJ (1973) *Radar Observations of the Atmosphere* (revised edn.). University of Chicago Press.

DIXON M and WIENER G (1993) TITAN: Thunderstorm identification, tracking, analysis and nowcasting - A radar-based methodology. *J. Atmos. Ocean. Tech.* **10**(6) 785-797.

DOVIAK RJ and ZRNIC DS (1984) *Doppler Radar and Weather Observations.* Academic Press, New York, USA.

MARSHALL JS and PALMER W (1948) The distribution of raindrops with size. *J. Meteorol.* **5** 165-166.

MOHR CG and VAUGHAN RL (1978) An economical technique for Cartesian interpolation and display of reflectivity factor data in three-dimensional space. *Proc. 18th Conf. on Radar Meteorol.*, Atlanta, Georgia. 490-496.

MATHER GK and TERBLANCHE DE (1994) Initial results from cloud seeding experiments using hygroscopic flares. *Proc. 6th WMO Sci. Conf. on Weather Modification*, Paestum, Italy. 687-690.

SEED AW (1992) Generation of a Spatially Distributed Daily Rainfall Database for Various Weather Modification Scenarios. Report to the Water Research Commission by the Directorate Hydrology. Department of Water Affairs and Forestry. WRC 373/1/92.

SEED AW (1993) On the interpolation of daily rainfields from gauge measurements. *Proc. 6th S. Afr. Hydrol. Symp.*, Pietermaritzburg. Vol. **I** 79-86.

TERBLANCHE DE (1996) A simple digital processing method to simulate linear and quadratic responses from a radar's logarithmic receiver. *J. Atmos. Ocean. Tech.* **13** (2) 533-538.

TERBLANCHE DE, HISCUTT FO and DICKS DJ (1994) The upgrading and performance testing of the Bethlehem weather radar. *S. Afr. J. Sci.* **90** 588-595.

VAN DER HOVEN AM and KROESE NJ (1995) An automated tipping bucket rain gauge calibrator. *Proc. 7th S. Afr. Natl. Hydrol. Symp.*, Grahamstown, SANCIAHS. 66.

VISSER PJM and LE ROUX E (1993) The radar network of the Weather Bureau. *Proc. 10th Annu. Conf., S. Afr. Soc. for Atmos. Sci.* **72**.